Received: 26 May 2020 | Revised: 4 September 2020 | Accepted: 11 September 2020

DOI: 10.1111/jpi.12696

ORIGINAL ARTICLE

Journal of Pineal Research
Molecular, Biological, Physiological and Clinical Aspects of Melatonin

WILEY

A novel role for the pineal gland: Regulating seasonal shifts in the gut microbiota of Siberian hamsters

Elyan K. Shor | **Shawn P. Brown** | **David A. Freeman**

Department of Biological Sciences, Center for Biodiversity Research, University of Memphis, Memphis, TN, USA

Correspondence
Elyan K. Shor, Department of Biological Sciences, Center for Biodiversity Research, University of Memphis, Memphis, TN, USA.
Email: ekshor@memphis.edu

Funding information
University of Memphis

Abstract

The gut microbiota plays a significant role in a variety of host behavioral and physiological processes. The mechanisms by which the gut microbiota and the host communicate are not fully resolved but include both humoral and direct neural signals. The composition of the microbiota is affected by internal (host) factors and external (environmental) factors. One such signal is photoperiod, which is represented endogenously by nocturnal pineal melatonin (MEL) secretion. Removal of the MEL signal via pinealectomy abolishes many seasonal responses to photoperiod. In Siberian hamsters (*Phodopus sungorus*), MEL drives robust seasonal shifts in physiology and behavior, such as immunity, stress, body mass, and aggression. While the profile of the gut microbiota also changes by season, it is unclear whether these changes are driven by pineal signals. We hypothesized that the pineal gland mediates seasonal alterations in the composition of the gut microbiota. To test this, we placed pinealectomized and intact hamsters into long or short photoperiods for 8 weeks, collected weekly fecal samples, and measured weekly food intake, testis volume, and body mass. We determined microbiota composition using 16S rRNA sequencing (Illumina MiSeq). We found significant effects of treatment and time on the abundances of numerous bacterial genera. We also found significant associations between individual OTU abundances and body mass, testis mass, and food intake, respectively. Finally, results indicate a relationship between overall community structure, and body and testis masses. These results firmly establish a role for the pineal gland in mediating seasonal alterations in the gut microbiota. Further, these results identify a novel neuroendocrine pathway by which a host regulates seasonal shifts in gut community composition, and indicates a relationship between seasonal changes in the gut microbiota and seasonal physiological adjustments.

KEYWORDS

gut microbiota, hamster, physiology, pineal gland, seasonal

1 | INTRODUCTION

The gut microbiota—defined as the community of microorganisms within the gastrointestinal tract[1,2]—has become an increasingly important area of research, as studies have shown that the microbiota plays significant roles in a variety of host behavioral and physiological processes.[3-5] The gut microbiota may have multiple beneficial effects associated with metabolism and immune function[4-6] but has also been linked to pathological conditions including inflammatory and immunological diseases, especially when in a dysbiotic state.[7] An increasing number of studies suggest that shifts in gut microbial community structure can lead to pathogenicity[8-10] and affect host metabolism.[11] Gut microbiota activity has also been linked to mammalian host behavior, including impacts on exploratory and motor behavior,[12-14] depression,[5,15] anxiety,[6,16-18] social interactions,[19-22] aggression,[23,24] and diet choice.[25,26] The microbiota can be altered by changes in either endogenous factors related to the host (such as stress[1]) or exogenous environmental factors (such as photoperiod[23,27]).

The mechanisms by which gut microbiota communicate with their hosts are not well resolved, but appear to include both humoral (eg, neurotransmitters secreted by gut microbes) and direct neural signaling via the vagus nerve.[2,4,13,28-31] Though many studies have focused on microbial regulation of host physiology and behavior,[2,5,6,31-33] there has been less focus on host regulation of the gut microbiota. The gut community appears to be sensitive to multiple signals from the host—including immune system signals[34] and stress hormones[31,35,36]—as well as environmental signals such as diet[37,38] and photoperiod.[23,27,39]

To understand the relationship between environment, host, and microbiota, it is necessary to determine the role of photoperiod on the profile of the gut community. A robust role for photoperiod in regulating both the hypothalamus-pituitary-adrenal (HPA) axis and the immune system has already been established in Siberian hamsters.[40-44] Given that the gut microbiota is closely tied to immune function and impacts neural function to regulate behavior and physiology, it is critical to understand the effects of photoperiod on the microbiota and to characterize the mechanisms underlying these relationships.

Siberian hamsters (*Phodopus sungorus*) are photoperiodic mammals that display robust seasonal changes in behavior and physiology, including responses of pelage color,[45] body mass,[46] immune function,[33] reproduction,[47] and aggression.[48] These seasonal changes are largely driven by the pattern of melatonin (MEL) release from the pineal gland.[49] MEL is produced by the pineal gland and is only secreted at night. The duration of MEL secretion is therefore directly proportional to length of night. In long, summer-like days, the duration of MEL is short, whereas in short, winter-like days, the duration of MEL is longer. The MEL signal communicates photoperiod information to a variety of targets throughout the body and brain.[50] As such, day length—and ultimately the time of year information—is encoded endogenously by rhythmic pineal MEL secretion.[51] Removal of the pineal gland (pinealectomy) abolishes many of the seasonal responses to photoperiod in Siberian hamsters, leaving intact those seasonal changes that are instead likely directly dependent on seasonal changes in circadian entrainment.[50]

This study investigates the role of the pineal gland in mediating the profile of the gut microbiota. Data from previous studies[23,27] indicate that the relative abundances of certain intestinal bacteria differed for Siberian hamsters housed in long- versus short-day lengths. This suggests that the gut microbiota responds to changes in photoperiod. Given that pineal MEL encodes information about photoperiod, we hypothesized that the pineal gland may play a role in determining the seasonal composition of the gut microbiota. Alternatively, seasonal changes in the gut microbiota may be among the limited number of seasonal responses that are pineal-independent.[50,52]

2 | METHODS

2.1 | Animals and housing

Male Siberian hamsters (*Phodopus sungorus*) (N = 40) were obtained from the University of Memphis breeding colony. Hamster pups were weaned at 18-21 days of age, after which they were housed in polypropylene cages (28 × 17 × 12 cm) with same-sex siblings (1-5 animals per cage). Cages contained wood-shavings bedding (Teklad Sani-chips 7090, Envigo, Madison, WI, USA) and shredded paper nesting material, and animals were given ad libitum access to food (Teklad Rodent diet 8640, Envigo, Madison, WI, USA) and filtered tap water. Ambient temperature in the room was maintained at 21°C ± 0.5, and relative humidity of 50 ± 2%. All animals were exposed to a 16:8-hr light-dark cycle (long day [LD]; lights off at 1800 Central Standard Time) until 3-4 months of age. Upon reaching 3-4 months, all animals were separated and individually housed within the same room. Following surgical procedures, 20 animals were transferred to a room with identical conditions, but with a 10:14-hr light-dark cycle (short day [SD]; lights off at 1800 Central Standard Time).

2.2 | Procedures

2.2.1 | Surgical procedures

20 male hamsters (3-4 months of age) were pinealectomized (PinX), and an additional 20 hamsters underwent sham

pinealectomy (treatments were randomly assigned). Briefly, each PinX animal underwent stereotaxic surgery in which the pineal gland was removed.[49] Sham pinealectomy operations involved cranial exposure, but the pineal gland was not removed.

Following surgery, animals were randomly assigned into one of four treatment groups: LD-PinX (LDP), LD-Sham (LDS), SD-PinX (SDP), and SD-Sham (SDS). Hamsters in the LD groups (N = 10 PinX, N = 10 sham) remained housed in long-day conditions (16L:8D photoperiod). Hamsters in the SD groups (N = 10 PinX, N = 10 sham) were transferred to short-day conditions (10L:14D photoperiod).

2.2.2 | Food intake and body mass

Food was weighed weekly, three hours prior to the dark phase, for seven weeks postsurgery. Food hoppers were topped or re-filled every five days. Each hamster was weighed (body mass in g ± 0.01 g) one week prior to surgery, as well as weekly for the duration of the study.

2.2.3 | Testicular measurements

Estimated testis volume (ETV) was used to determine the response to photoperiod.[53] ETV was calculated by multiplying testis length by the width squared. Beginning prior to surgery (Week 0), testis measurements were obtained using analog calipers, while animals were under light anesthesia (3% isoflurane and medical oxygen at a flow rate of 3 L/min). ETV measurements were recorded weekly for the duration of the study. Testes were surgically removed and weighed at the termination of the study for final determination of paired testis mass (PTM). For ease of reference, all testis measurements (both ETV and PTM) will be jointly referred to as PTM. A reduction in ≥ 30% PTM by Week 8 was classified as gonadal regression.[44,53] Animals that failed to exhibit ≥ 30% decreases in testis size were classified as SD nonresponders and excluded from subsequent analyses.

2.2.4 | Sample collection

Fresh fecal samples were collected from each animal weekly (on Weeks 0, 2, 4, and 8), at the same time (0900 Central Standard Time) and day of the week (Figure 1). We used a repeated sampling approach to better understand timing of induced bacterial community shifts with treatments. Terminal samples were collected on the last day of the eighth week postsurgery. Samples were collected by removing animals from their home cage and holding above a sterile container until fecal deposition. All pellets were transferred aseptically into individual 1.5-mL microcentrifuge tubes and were stored at −80°C until processing.[24]

All experimental procedures and husbandry were approved by the University of Memphis Animal Care and Use Committee (Protocol # 815) and comply with the criteria established by the NIH Guide for the Care and Use of Laboratory Animals.

2.3 | DNA extractions and library preparation

Genomic DNA was extracted from 152 fecal samples (each sample = 2-4 fecal pellets per animal) using Soil DNA Extraction Kits (IBI Scientific, Dubuque, IA, USA) following the manufacturer's protocol. DNA was quantified using a NanoPhotometer N60 (Implen, München, Germany). To maximize sample intercomparability, DNA was normalized to a 50 ng/μL working concentration prior to amplicon generation.

Bacterial amplicon libraries were generated by amplifying the 16S (V4) ribosomal RNA (rRNA) region. The V4 region of the rRNA gene repeat was amplified in a two-step process using the forward primer nexF-N[3-6]-515f and the reverse primer nexR-N[3-6]-806r.[54-56] These forward and reverse primer constructs include the following: bacterial primers (515f and 806r), Nextera forward (nexF) and reverse (nexR) sequencing primers, and four identical primers comprised of ambiguous nucleotides mixed to equal molarity (N[3-6]) to increase sequence variation.

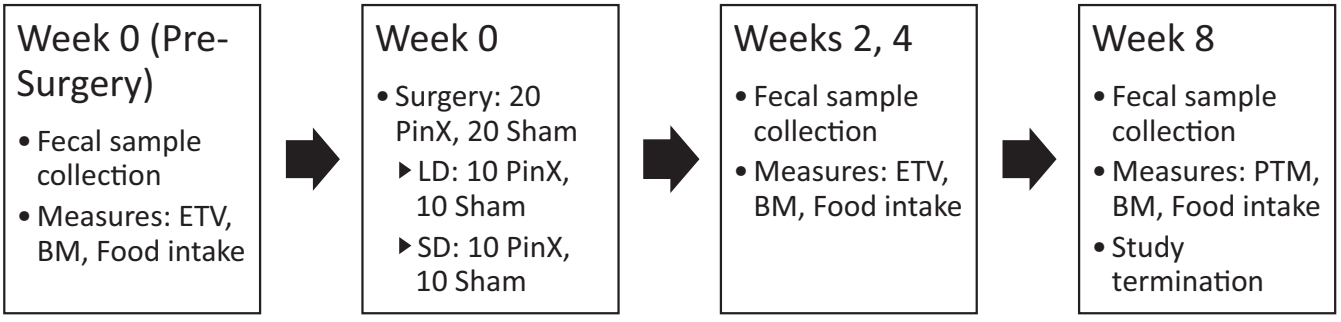

FIGURE 1 Study and Sampling Design. ETV: estimated testis volume, BM: body mass, PinX: pinealectomy, PTM: paired testis mass

Libraries were constructed following Brown, et al[56] Primary PCRs were conducted in triplicate, in 25 μL reactions consisting of 2 μL (100 ng) DNA template, 2.5 μL of each forward and reverse primer (1.0 μmol/L concentration), 12.5 μL 2X Phusion Green Hot Start II High-Fidelity PCR Master Mix (Thermo Fisher Scientific, Waltham, MA, USA), and 8 μL molecular grade water. PCR parameters consisted of 98°C for 30 s, 25 cycles of 98°C for 20 s, 52.5°C annealing temperature for 30 s, 72°C for 40 s, and final extension at 72°C for 10 min. All ramp rates were 1°C/s. Following primary PCR, all samples were visualized using gel electrophoresis (1.5% agarose *w*:*v* in TBE).

Secondary PCRs were conducted in 25 μL reactions using 12.5 μL PCR Master Mix (as above), 2.5 μL of primary PCR product that was used as template DNA, 7.5 μL molecular grade water, and 2.5 μL barcoded secondary primers. The secondary primers consisted of forward primers including the P5-i5-overlap and reverse primers P7-i7-overlap, where P5 and P7 represent the Illumina Adaptor sequences, i5 and i7 are 8 bp unique barcodes (MIDs), and the overlap is the partial nexF and nexR sequence that acts as the annealing site for the secondary PCR.[55] PCR parameters were 98°C for 30 s, 8 cycles of 98°C for 20 s, 50°C for 30 s, 72°C for 40 s, and final extension at 72°C for 10 min.[56] The final amplicon constructs produced after 32 cycles were P5-i5-nexF-N[3-6]-515f-V4-806r-N[3-6]-nexR-i7-P7. Following secondary PCR, all samples were visualized using gel electrophoresis. A negative control consisting of molecular grade water was used through extraction and library prep and remained visually free from contamination throughout.

Secondary PCR products were cleaned using Axygen Axyprep Mag PCR beads (Axygen Bioscience, Union City, CA, USA). Cleaning followed the manufacturer protocol but was modified to use a 1:1 bead solution to reaction volume ratio.[57] Cleaned PCR products were quantified using Qubit 3.0 fluorometric assays (dsDNA HS Assay Kit; Thermo Fisher Scientific, Waltham, MA, USA), and pooled to equal mass per sample. This library was sequenced in a single run on Illumina MiSeq (300PE) at the Kansas State University Integrated Genomics Facility (Manhattan, KS, USA). Paired fastq files for all 152 samples were generated by using the unique combinations of i5 and i7 sequences to demultiplex the raw sequence data (Table S1). All sequences are deposited in the Sequence Read Archive (SRA) at NCBI under the following accessions: BioProject PRJNA641652, BioSamples SAMN15369034 - SAMN15369184.

2.4 | Bioinformatics

Sequence data were processed with the program mothur[58] (RRID:SCR_011947; http://www.mothur.org), generally following the MiSeq SOP[59] with modifications. The forward and reverse sequences were contiged, screened, and culled to remove sequences with ambiguous bases or sequences with more than 10 homopolymers. Sequences were then merged into a single fasta file, and primers were trimmed using the program Cutadapt[60] (v.2.8; RRID:SCR_011841; http://code.google.com/p/cutadapt). Retained sequences were aligned against the SILVA reference alignment (release 132; RRID:SCR_006423; www.arb-silva.de), and off-target sequences were filtered and excluded. Sequences were preclustered[61] and screened for chimeras (VSEARCH)[62] utilizing implementations within mothur. Sequences were taxonomically classified using a Naïve Bayesian Classifier[63] against the RDP training set (bacteria; v.10; RRID:SCR_006633); nonbacterial lineages were culled, and distance matrices (not punishing terminal gaps) were generated. Sequences were clustered into operational taxonomic units (OTUs) using OptiClust at a 97% similarity threshold.[64] Taxonomic identifications for each OTU were assigned based on the most representative sequence (centroid). To reduce the potential of inclusion of suspect or noninformative OTUs, we culled OTUs with fewer than 10 sequences globally.[65,66] OTUs that did not have 100% bootstrap support at the phylum level were confirmed manually using BLASTn (NCBI; RRID:SCR_001598; http://blast.ncbi.nlm.nih.gov/Blast.cgi) against GenBank (nr/nt). We utilized iterative subsampling (1000 iterations) to calculate relative OTU richness (S_{obs}), diversity (Compliment of Simpson's diversity index; 1-*D*), and evenness (Simpson's Evenness, E_D) to maximize comparability between samples.[56] Samples were queried at a subsample depth of 5000 sequences per sample. The resulting average diversity values were used in subsequent analyses.

2.5 | Statistical analyses

Weekly body mass (BM) measurements for each individual were calculated as a percent of BM relative to baseline BM ([Weekly BM]/[100]). Weekly food intake for each individual was calculated as grams of food consumed per gram of BM. Body mass, food intake, and testicular measures were analyzed using repeated-measures analysis of variance (ANOVA) models against the four levels of treatment (LDP, LDS, SDP, and SDS), time, and their interactions using the program JMP (JMP Pro v.14.1, SAS Institute Inc, Cary, NC, USA). Body mass and testis mass data were transformed using Box-Cox functions prior to analysis in order to meet the ANOVA assumption of normality ($\lambda = 2$ for BM, and $\lambda = 1.69$ for PTM). Tukey's HSD was performed to determine treatment differences, where applicable.

To investigate whether bacterial communities differed by treatments across time, we used a series of PERMANOVAs[67] on average Bray-Curtis (BC) dissimilarity values (average BC values over 1000 iterations of 5000 subsampled sequences

per experimental unit). We aimed to elucidate whether treatments facilitated a shift in the gut microbiota and whether this effect, if any, was consistent across sampling dates. To visualize community differences at Week 8, principal coordinates analysis (PCoA) was conducted (as implemented in mothur) using BC dissimilarity values (subsampled as above), and a contour plot (nonparametric density) was generated using JMP Pro. Additionally, we were interested in whether communities differed within a repeatedly sampled hamster differed with treatments and over time. To examine this, we used the BC dissimilarity values (as above) to investigate how community similarity within each hamster changes with treatments by constraining our analysis to only within-subject comparisons, but accounting for all within-hamster comparisons across time (n = 6). We linearly regressed these pairwise dissimilarity values against the same pairwise changes in BM, PTM, and food intake (within-subject). This allows for variation in community analyses to account for individual differences in physiological responses, thus controlling for individual variability.

Additionally, previous investigations[23,27] indicate that individual OTU responses play a large role in explaining differential host-derived effects on the microbiota[23,27,36-39,68-70] (ie, effect of treatment on microbiota), as well as effects of the microbiota on host physiology.[9,11-13,15,16,31,71] To investigate individual OTU responses to treatments, we used two-way repeated-measures ANOVAs on OTU relative abundance values (for the 100 most abundant OTUs, which represents greater than 78% of all obtained sequences) against time, treatment, and the treatment-by-time interaction, with post hoc Tukey's HSD tests where applicable. OTU abundance data were logit-transformed prior to analyses. Two-way repeated-measures ANOVAs with Tukey's HSD were also used to analyze OTU abundance by taxonomic rank (relative abundance at the phylum and genus levels). Further, at the terminal sampling date (Week 8), we used a combination of one-way ANOVA and linear discriminant analysis [LDA] effect size (LEfSe)[72] to identify OTUs that were differentially abundant across treatment groups. In addition, we were interested in whether individual OTU abundances (100 most abundant) were responsive to somatic measures; to examine this, OTU relative abundances (logit-transformed) were regressed against BM, PTM, and food intake over time. Where relevant, we corrected for multiple comparisons using the Benjamini-Hochberg[73] procedure (FDR = 0.25) and reported significant p-values both pre- and post-adjustment.

3 | RESULTS

3.1 | Exclusions

One individual from the SDS group was classified as a nonresponder and was excluded from analyses. One pinealectomized hamster from the SDP group was unsuccessful (the hamster exhibited the typical body mass and testicular photoperiodic responses of a pineal-intact hamster); therefore, this individual was excluded from analyses. The final group totals after these exclusions were as follows: LDS = 10, LDP = 10, SDS = 9, and SDP = 9 hamsters. After exclusions, the total number of fecal samples analyzed was 152.

3.2 | Sequencing

After sequence quality control, including exclusion of rare OTUs, we retained ~1.2 million sequences, representing demarcated 3,409 OTUs. The communities were dominated by the phyla Bacteroidetes (51.5% of OTUs) and Firmicutes (45.3% of OTUs). The 100 most abundant OTUs represented 78% of all sequences (63.2% Firmicutes and 31.5% Bacteroidetes) (Table S2).

3.3 | Diversity estimators

There was a difference in relative OTU richness with the interaction of treatment and time ($F_{3,144} = 2.75$, $P = .045$). LDP animals had higher observed OTU richness than SDP animals ($F_{1,144} = 5.35$, $P = .022$). There were no significant differences in diversity ($F_{3,144} = 2.00$, $P = .116$) or evenness ($F_{3,144} = 1.83$, $P = .144$).

3.4 | Body mass, food intake, and testes mass

The pattern of BM change was dependent on both photoperiod and pineal status ($F_{3,142} = 17.15$, $P < .0001$); thus, animals in both of the SD groups lost more mass than the LDP group ($t = 5.69$, $P < .0001$), and SDS animals lost significantly more mass than LDS animals ($t = -2.11$, $P = .037$) (Figure 2A) (means: SDP = 45.51 ± 2.50%, SDS = 36.55 ± 2.50%, LDP = 56.51 ± 2.37%, and LDS = 50.13 ± 2.37%, where transformed values represent final BM as a percent of baseline BM [100%]). There was also a significant treatment by time effect on BM ($F_{3,142} = 16.98$, $P < .0001$), where LDP had significantly higher BM than SDS ($t = 5.21$, $P < .0001$).

Food intake varied as a function of time ($F_{1,142} = 5.40$, $P = .022$), with animals eating more on Week 8 than Week 0 ($t = 2.32$, $P = .022$). There was no significant effect of treatment ($F_{3,142} = 2.46$, $P = .065$) or the interaction of treatment by time ($F_{3,142} = 1.33$, $P = .266$) on food intake.

PTM differed among groups ($F_{3,142} = 27.98$, $P < .0001$), with SDS animals exhibiting significantly greater

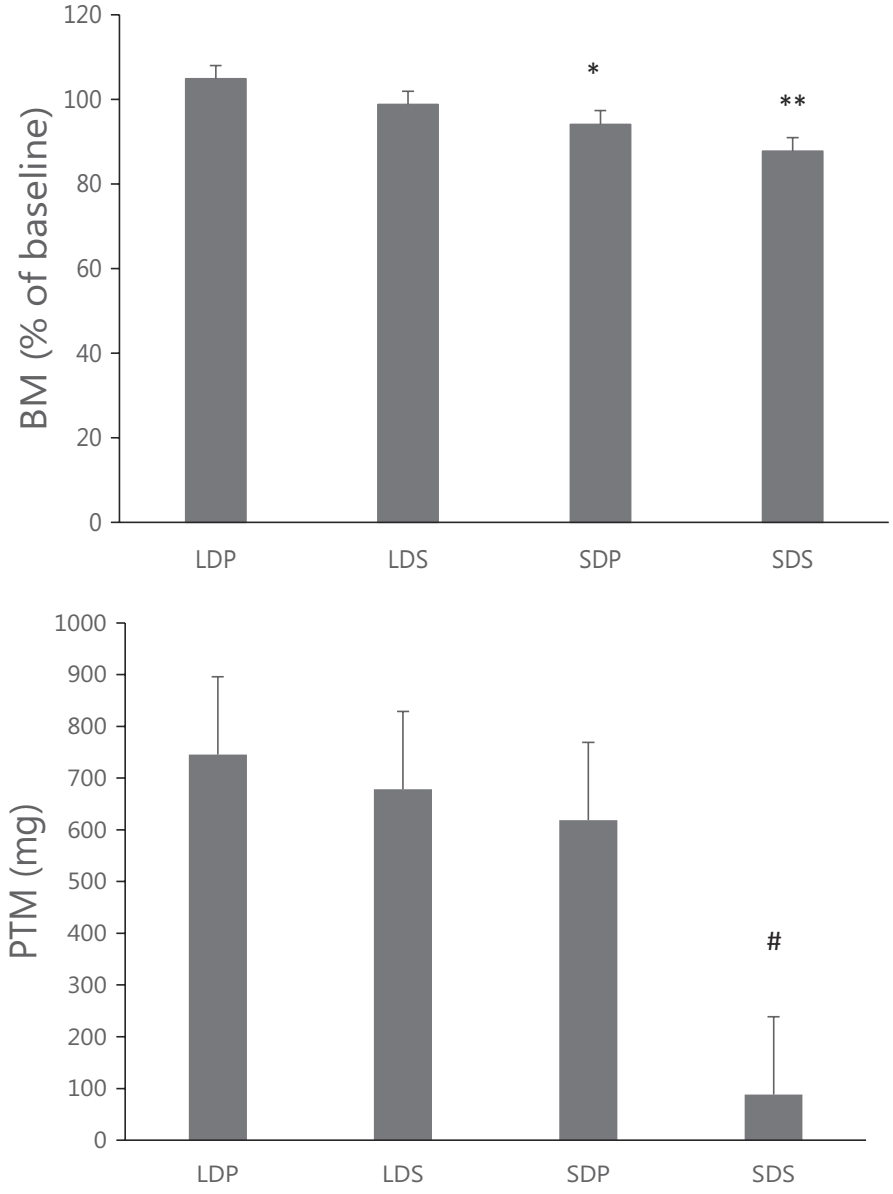

FIGURE 2 Body mass (A) and paired testes mass (B) on Week 8. BM: body mass, expressed as percent change in BM as compared to baseline BM. PTM: paired testes mass. Graphs are based on raw values (% of baseline), while statistical analyses are transformed values (Box-Cox, see Methods). *$P < .001$. **$P = .037$. #$P < .0001$

reduction in testicular mass (mean = 21.41 ± 54.60 mg) as compared to all other groups on Week 8 (Figure 2B) (means: LDS = 563.83 ± 51.80, LDP = 533.25 ± 51.80, SDP = 404.97 ± 54.60 mg).

3.5 | OTU abundance—all weeks

The results indicate that treatment, time, and their interaction significantly affect the abundance of several OTUs (Table 1).

Results from post hoc analyses indicate that treatments do not uniformly affect OTU abundances (Table 1a). For example, SDP had less *Muribaculum* (OTU 92) than LDS ($t = -3.25$, $P = .002$), as well as less *Hungatella* (OTU 95) than SDS ($t = -3.25$, $P = .0015$). LDS also had less *Lactobacillales* than SDS ($t = -3.34$, $P = .0011$). For a full report of differences by treatment group, see Table S3.

OTU abundance was also significantly affected by time. Except for one (OTU 174, $t = 3.32$, $P = .002$), all significant OTUs (from within the top 100) decreased over time (Table 1b).

Finally, the interaction of treatment and time significantly affected OTU abundances. There were several significant differences in OTU abundances between groups. SDP animals had significantly more *Prevotella*, *Clostridium*, and one OTU belonging to the genus *Fusimonas* than SDS animals over time. However, SDP had significantly lower abundances of *Desulfovibrio* and another OTU of *Fusimonas* than SDS over time. *Lactobacillus* was more abundant in LDP versus SDS over time, whereas the opposite was true for another OTU of *Prevotella* (Table 1c).

TABLE 1 Effect of treatment (a), time (b), and the interaction of treatment and time (c) on OTU abundance, Weeks 0 through 8

Effect	Phylum	Order	Genus	OTU no.	F_{df} (s)	*P*-value(s)	Direction
(a) Treatment	Actinobacteria	Bifidobacteriales	*Bifidobacterium*	64	$F_{3,21.6} = 3.410$	.036	B > C
	Bacteroidetes	Bacteroidales	*Muribaculum*	92, 156	$F_{3,135} = 4.434$, $F_{3,29.2} = 3.193$	.005[b], .038	92: B,D > C 156: B > C
	Firmicutes	Clostridiales	*Hungatella*	95, 134, 192	$F_{3,135} = 4.434$, $F_{3,33.7} = 4.659$, $F_{3,36.4} = 3.416$	.005[b], .008[b], .027	95: A,D > C 134: A > B 192: A > B,C,D
		Lactobacillales	*Lactobacillus*	139	$F_{3,136} = 5.217$	.002[b]	B,D > A
(b) Time	Bacteroidetes	Bacteroidales	*Prevotella*	182	$F_{1,83.4} = 4.295$	.041	Dec
			Muribaculum	17, 84, 100, 107, 174	$F_{1,111.9} = 6.759$, $F_{1,135} = 6.604$, $F_{1,108} = 4.511$, $F_{1,76.1} = 4.270$, $F_{1,58} = 11.030$	.011, .011, .036, .042, .002[b]	17-107: Dec 174: Inc
	Candidatus Saccharibacteria	Candidatus Saccharibacteria	*Candidatus Saccharibacteria*[a]	16, 24	$F_{1,110.8} = 5.500$, $F_{1,110.7} = 4.960$	.021, .028	Dec (all)
	Firmicutes	Clostridiales	*Acetatifactor*	74	$F_{1,107.1} = 5.353$	.023	Dec
			Clostridium XIVa	41, 85, 162	$F_{1,104.1} = 5.181$, $F_{1,94.7} = 8.207$, $F_{1,99} = 5.903$	.025, .005[b], .017	Dec (all)
			Flavonifractor	73	$F_{1,106.3} = 4.138$	.044	Dec
		Lactobacillales	*Lactobacillus*	8	$F_{1,111.6} = 11.845$	.001[b]	Dec
(c) Treatment x Time	Bacteroidetes	Bacteroidales	*Prevotella*	21, 182	$F_{3,111.1} = 5.210$, $F_{3,80.8} = 2.756$	.002[b], .048	21: C > D 182: D > A
	Firmicutes	Clostridiales	*Clostridium*	119	$F_{3,80.1} = 4.150$	.009[b]	C > D
			Fusimonas	102, 106	$F_{3,108.9} = 2.806$, $F_{3,100.5} = 3.647$	.043, .015	102: D > C 106: C > D
		Lactobacillales	*Lactobacillus*	105	$F_{3,86.5} = 3.112$	.03	A > D
	Proteobacteria	Desulfovibrionales	*Desulfovibrio*	43	$F_{3,99.4} = 4.350$	.006[b]	D > C

Note: Direction column indicates significant differences by treatment (a, c) or changes across time (b) (A: LDP, B: LDS, C: SDP, D: SDS, Dec: decreasing over time, Inc: increasing over time). *F*-ratios with degrees of freedom and P-values each correspond to the individual OTU numbers listed (separated by commas). Denominator partial *df* based on Kenward-Roger first-order approximations with Kacker-Harville corrections.

[a]OTUs 16 and 24 could not be classified at the genus level.

[b]Significant after Benjamini-Hochberg correction with FDR = 0.25.

3.5.1 | OTU abundance—all weeks—taxonomic Rank

The repeated-measures ANOVA to analyze the abundance of bacteria by taxonomic rank indicate significant effects of time, and the treatment-by-time interaction, at the phylum level. There was a significant effect of the treatment-by-time interaction on the phyla Bacteroidetes ($F_{3, 34.3} = 3.562$, $P = .0166$) and Firmicutes ($F_{3, 108.6} = 3.603$, $P = .0158$). There was a significant effect of time on the phylum Candidatus Saccharibacteria ($F_{1, 108.7} = 5.303$, $P = .0232$). Partial denominator degrees of freedom are based on Kenward-Roger first-order approximations with Kacker-Harville corrections. Treatment, time, and their interaction all had significant effects at the genus level—overall, there were significant effects on 20 genera, representing 6 phyla (see Table S4 for results at the genus level).

3.6 | OTU abundance—Week 8

We investigated OTU abundances in two ways: one-way ANOVA and LEfSe analysis. As both statistical approaches test for differential OTU abundances and as there was overlap in genera enriched, results from both tests are presented together (Table 2). Results of ANOVAs on OTU abundances (top 100 OTUs) with treatment in Week 8 indicate that two common OTUs, both in the genus *Prevotella*, were enriched in the SDP group. Further, LEfSe analysis indicated an additional OTU (genus *Prevotella*) enriched in SDP, as well as two other OTUs enriched in LDP and SDS (*Helicobacter* and *Lachnospiraceae*, respectively; Table 2). Week 8 treatment differences in relative abundances of genera (including *Prevotella*) are illustrated in Figure 3A.

Even though there was no evidence for major community-wide differences by treatment on Week 8 (see PERMANOVA and Bray-Curtis section, below), PCoA visualization indicates that there are differences by treatment which were driven by changes in the relative abundances on individual OTUs or genera (Figure 3A; Table 2). We can see in our contour plot of PCoA loadings that the relative abundances of genera within SDP and SDS groups were particularly distinct (Figure 3B).

3.7 | Effect of OTUs on somatic measures

There were many significant associations between individual OTU abundances with BM, PTM, and/or food intake. The significant correlations were largely with members of the phyla Firmicutes and Bacteroidetes. The OTUs that were significantly correlated with BM were mostly members of the orders Clostridiales and Bacteroidales (Table 3a). Most of the OTUs that affected PTM were within the Bacteroidales (Table 3b). Finally, several OTUs significantly affected food intake (Table 3c).

3.8 | PERMANOVA and Bray-Curtis

PERMANOVA results indicated significant differences in community structure by treatment, overall ($F_{3,144} = 1.51$, $P = .022$). However, when analyses were separated by time, treatment effects were not significant (W0: $F_{3,34} = 0.94$, $P = .566$; W2: $F_{3,32} = 0.93$, $P = .566$; W4: $F_{3,33} = 1.25$, $P = .116$; W8: $F_{3,33} = 0.89$, $P = .633$). This confirms that at the onset of this experiment, prior to surgery, initial gut communities were indistinguishable from each other.

BC was significantly affected by BM ($F_{7, 199} = 2.66$, $P = .012$; Figure 4A). As hamster BM increased over time, there was more dissimilarity in gut communities, regardless of treatment ($t = 2.58$, $P = .011$). This suggests a relationship between lack of gut community variation and the maintenance of body mass. BC is significantly affected by PTM over time ($F_{7, 199} = 2.66$, $P = .012$; Figure 4B). There was a significant interaction between treatment and PTM ($F_{3, 199} = 2.75$, $P = .044$): the larger testes of the LDS animals were associated with less community dissimilarity, as compared to SDS animals ($t = -2.67$, $P = .008$). There were no significant differences in the other groups (LDP vs SDS: $t = 1.77$,

TABLE 2 Effect of treatment on OTU richness (top 100) on Week 8

OTU no.	Genus	Enriched Treatment Group	F_{df}	LDA	*P*-value
4	*Prevotella*	SD-PinX	$F_{3,34} = 3.045$	–	.042
21	*Prevotella*	SD-PinX	$F_{3,34} = 3.368$	–	.030
182	*Prevotella*	SD-PinX	–	3.597	.013
55	*Helicobacter*	LD-PinX	–	3.840	.020
102	*Lachnospiraceae*[a]	SD-Sham	–	3.500	.013

Note: Analyses were either ANOVA (F-ratio) or LEfSe (LDA).

Abbreviations: SD, short day; LD, long day; PinX, pinealectomy.

[a]OTU 102 could not be classified at the genus level.

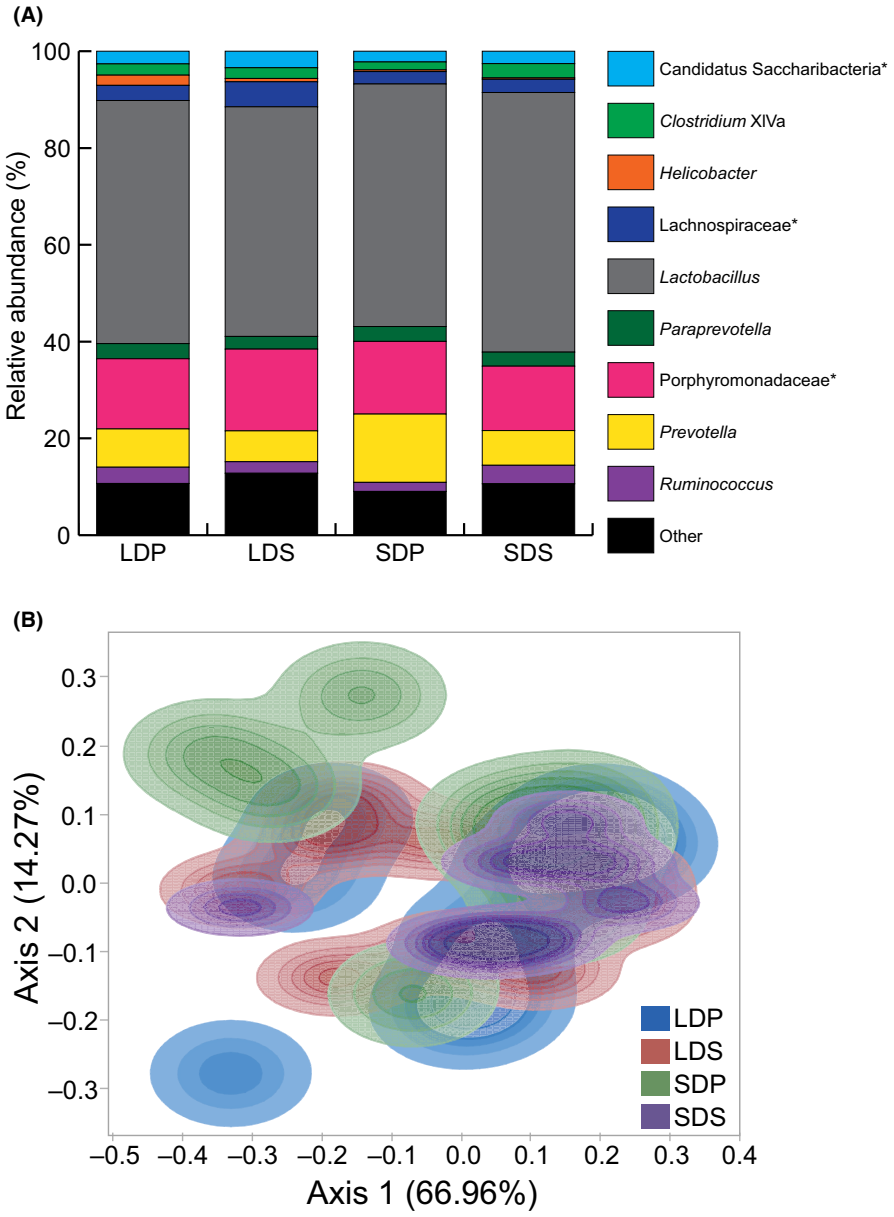

FIGURE 3 Relative abundances of genera (A) and gut community differences by treatment (B) across treatments for Week 8. A: relative abundances of top nine genera (with remaining genera grouped as Other); *OTUs could not be classified at the genus level. B: Contour plot of principal coordinates analysis (PCoA) loading values for the first two axes, with R^2 values for each axis presented parenthetically, demonstrating that short-day pinealectomized (SDP) gut communities are largely different from short-day sham (SDS); darker contours indicate close clustering of PCoA points for each treatment

$P = .078$; SDP vs SDS: $t = 0.83$, $P = .405$). This suggests that communities tend to be more similar to each other in animals that maintain large testis size. While food intake and BC tests indicated significant associations ($F_{7,199} = 2.26$, $P = .013$), we observed no significant individual treatment effects; additional research is needed to confirm this association.

4 | DISCUSSION

Recent studies have established that there are seasonal rhythms in the gut microbial community in Siberian hamsters.[23,27] Our present findings provide an alternative hypothesis regarding the mechanism(s) through which photoperiod drives other seasonal rhythms in physiology and behavior. Given that the gut microbiota has been implicated in many physiological and behavioral functions, pineal-dependent alterations in the gut microbiota may serve as a mechanism to affect downstream seasonal responses (ie, energetics, food intake, and social and aggressive behaviors). Thus, understanding the mechanism by which photoperiod influences the gut microbiota is of significant interest. The purpose of this study was to investigate the role of the pineal gland in shaping the seasonal profile of the gut microbiota. We hypothesized that the pineal gland is necessary for the expression of seasonal alterations in the composition of the gut microbiota. To test this, we placed pinealectomized and intact hamsters into long or short photoperiods for eight weeks, collected weekly fecal samples, and measured weekly food intake, testis volume, and body mass. We found significant effects of treatment on many bacterial genera. We also found significant associations between individual OTU abundances and BM, PTM, and food intake. Finally, our results indicate a relationship between overall community structure, and body

TABLE 3 Significant effects of OTUs on somatic responses: body mass (a), paired testes mass (b), and food intake (c)

Somatic Measure	Phylum	Order	Genus	OTU no.	*P*-value(s)	r^2 adjusted value(s)	*t*-ratio(s)
(a) Body mass	Bacteroidetes	Bacteroidales	*Barnesiella*	67	.004[b]	0.053	−2.89
			Muribaculum	79, 84, 91, 174	.001[b], .004[b], .029, .014	0.076, 0.051, 0.026, 0.058	3.58, 2.94, 2.21, −2.51
	Firmicutes	Clostridiales	*Paraprevotella*	186	.045	0.024	2.02
			Blautia	164	.008[b]	0.045	2.69
			Clostridium XlVa	41, 162	.001[b], .046	0.069, 0.022	3.42, 2.01
			Flavonifractor	38	.041	0.021	2.06
			Hungatella	118, 134	.013, $P < .001$[b]	0.047, 0.079	2.54, 3.60
			Kineothrix	137, 169	.043, .002[b]	0.064, 0.058	2.08, 3.10
			Pseudoflavonifractor	165	.028	0.029	2.22
	Proteobacteria	Campylobacterales	*Helicobacter*	99	.007[b]	0.051	2.74
(b) Paired testis mass	Bacteroidetes	Bacteroidales	*Barnesiella*	97, 136	.038, .033	0.025, 0.025	2.09, −2.15
			Muribaculum	48, 84	$P < .001$[b], .025	0.090, 0.028	3.97, 2.26
	Candidatus Saccharibacteria	Candidatus Saccharibacteria	*Candidatus Saccharibacteria*[a]	16	.022	0.029	2.32
	Firmicutes	Clostridiales	*Clostridium*	119	.041	0.029	2.07
(c) Food intake	Bacteroidetes	Bacteroidales	*Muribaculum*	81, 84, 91	.019, .032, .013	0.032, 0.025, 0.036	2.38, −2.17, −2.52
	Candidatus Saccharibacteria	Candidatus Saccharibacteria	*Candidatus Saccharibacteria*[a]	16	.013	0.035	−2.53
	Firmicutes	Clostridiales	*Hungatella*	118	.003[b]	0.071	−3.09
			Faecalicatena	181	.002[b]	0.104	−3.25
		Lactobacillales	*Lactobacillus*	52, 160	.045, .034	0.020, 0.025	−2.02, −2.15

Note: P-values and r^2 adjusted values each correspond to the individual OTU numbers listed (separated by commas).

[a]OTU 16 could not be classified at the genus level.

[b]Significant after Benjamini-Hochberg correction with FDR = 0.25.

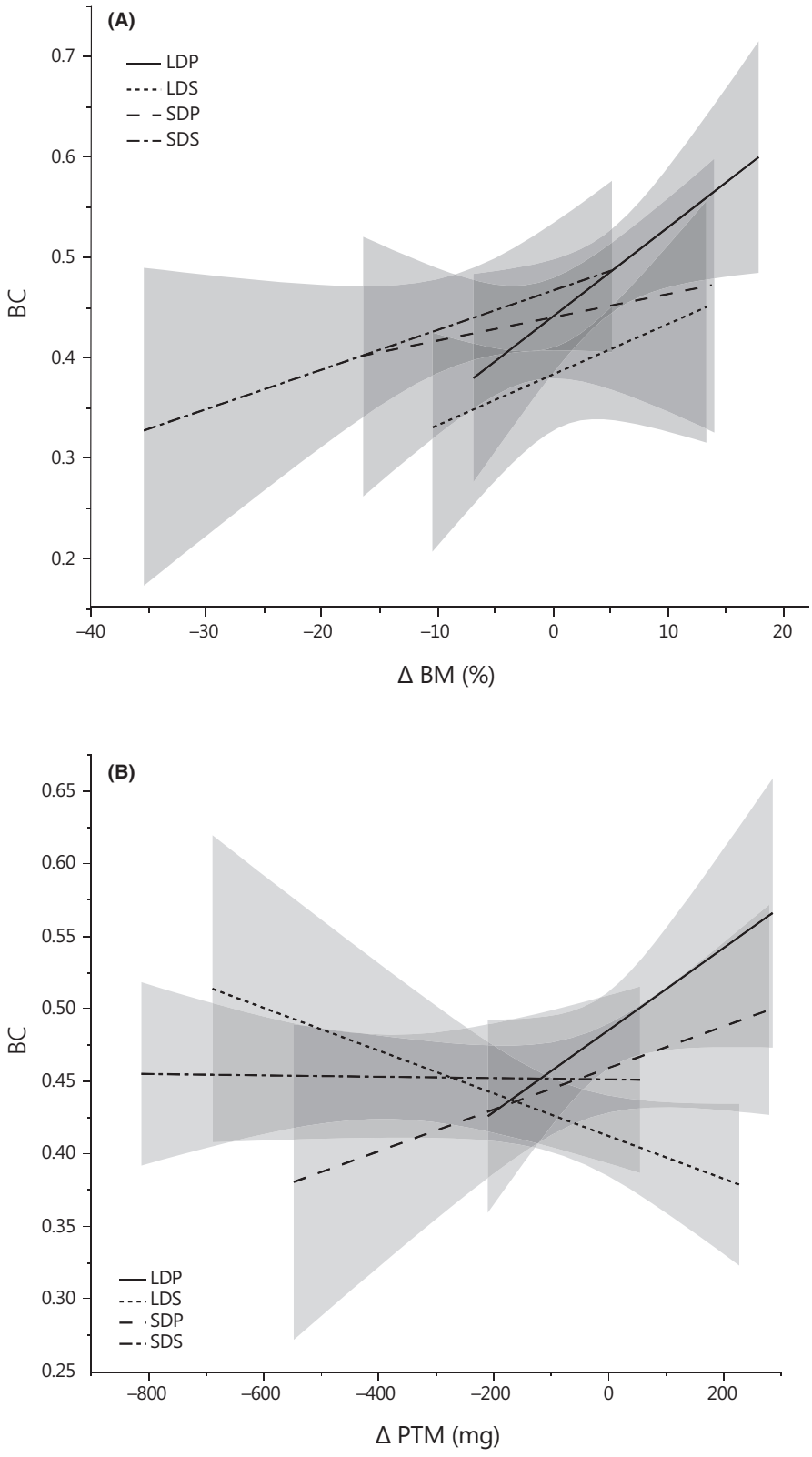

FIGURE 4 Association between body mass (A) and paired testes mass (B) with Bray-Curtis dissimilarity values. BC was significantly associated with changes in BM ($F_{7, 199} = 2.66$, $P = .012$) and PTM ($F_{7, 199} = 2.66$, $P = .012$) over time. Shaded area surrounding each line represents confidence interval. BM, body mass; PTM, paired testes mass; BC, Bray-Curtis dissimilarity

and testes masses. These results support our hypothesis, and firmly establish a role for the pineal gland in mediating some seasonal alterations in the gut microbiota.

There was a relationship between photoperiod, pineal status, and a number of bacterial genera. For example, the genus *Hungatella*, which is associated with carbohydrate metabolism and energy harvest,[74] was significantly enriched in the LDP group. As another example, the genus *Prevotella* was enriched in SDP animals on Week 8, and was significantly affected by treatment, as well as the interaction of treatment and time. Previous studies have indicated that *Prevotella* is associated with improved glucose tolerance

(mouse model),[75] decreased adiposity (human model),[68] and inflammatory responses (human model).[76,77] Whether *Prevotella* or *Hungatella* affected the seasonal physiology of hamsters in the context of this study is unclear, as we did not measure these responses; furthermore, the effects of the bacteria within these genera vary by species.[78,79] However, it is clear from our results that both photoperiod and pineal status affect the abundance of various bacteria, and this shift in abundances may be linked to seasonal shifts in physiology.

Our results reveal significant correlations between gut bacteria and physiological responses. For example, body mass was correlated with the phyla Bacteroidetes and Firmicutes. Interestingly, both phyla are often involved in carbohydrate metabolism.[80] The products of carbohydrate fermentation provide the host with energy, but they also communicate with the host neuroendocrine system to alter energy metabolism.[81-84] Prior research in human and animal models established that the gut microbiota influences body weight,[71,81,85-87] energetics,[71,81] and fat storage.[87] These are all measures that are seasonally regulated in Siberian hamsters by a complex system involving the pineal gland and other endocrine, neural, and genetic factors.[88-90] Taken together, the pineal gland may drive seasonal changes in gut bacteria that, in turn, contribute to seasonal changes in physiology and behavior such as body mass and food intake in the host.

Photoperiod is represented endogenously by pineal MEL secretion. Pineal MEL communicates information about day length to induce seasonal responses in behavior and physiology in targets throughout the mammalian body. Removal of the pineal gland via pinealectomy abolishes many seasonal responses to photoperiod. The results of this study extend those observations to include pineal-dependent seasonal shifts in the gut microbiota, as the abundances of certain bacteria significantly differed in pinealectomized versus intact animals. Investigation of the relationship between the brain and the microbiota is still in its early stages.[32] Communication along the gut-brain axis is complex, and although it is established that endocrine, neural, metabolic, and immune factors are all involved,[32,91,92] there is still much unknown regarding both the network that connects these factors and the roles of individual tissues/factors. Many gut-brain axis studies emphasize the effects elicited by the microbiota on the brain and body, particularly with regard to mood and behavior.[6,18,30,93-95] However, communication along the gut-brain axis is bidirectional,[4] so it is important to characterize the relationship from the perspectives of both bacteria (gut) and host (brain). There is already evidence of diurnal variation in the gut microbiota,[69,70,96-99] evidence that gut microbes influence host circadian clock functions,[34,96,97,100-103] and evidence that the circadian rhythms of the microbiota are regulated by the rhythms of the host.[39,70,96,98] However, the role of the host in seasonal rhythmicity of the gut microbiota has not been established until now. The current study indicates the presence of a "top-down" system of control, whereby information about photoperiod communicated by the brain (pineal gland) exerts influence on the gut community. These results are the first to show that at least some seasonal shifts in microbiota are pineal-dependent.

Extrapineal MEL is synthesized by various cell types in the gastrointestinal (GI) tract of birds and mammals.[104-107] The levels of gastrointestinal melatonin (GI-MEL) are 10-400 times higher than in the pineal and serum.[108-110] However, the mode of release of GI-MEL is not circadian;[105] rather, it appears that MEL is released in response to food intake.[104] Further, some foods themselves are rich in MEL, and thus likely contribute to the high levels of MEL present in the GI tract.[105,107,111] Although the role of GI-MEL in the digestive tract is not fully understood, evidence indicates that auto- and paracrine actions of GI-MEL include stimulation of GI motility,[104,105,112,113] transmembrane transport of water, ions, and electrolytes,[105] and its antioxidant effects may be gastroprotective.[105,111] The activity of at least one enteric bacterium has also been shown to respond to GI-MEL.[106,107] There is currently no evidence that GI-MEL enters the systemic circulatory system,[106] and previous studies indicate that GI-MEL synthesis is not affected by pinealectomy.[105,108] Thus, the results of the present study are likely independent of GI-MEL as the only intervention was to remove the pineal gland, leaving GI-MEL signaling intact in all groups.

The overall results of this study confirm and extend previous work establishing seasonal differences in the Siberian hamster gut microbiota. While previous results[23,27] indicate significant differences by photoperiod in the relative abundances of certain members of the microbiota, the significant bacteria in those studies are different than those in the present study. Diet, environment, and genetics play important roles in shaping the profile of the gut microbiota,[37,38] so it is therefore not surprising to see community differences across independent hamster colonies that are housed in different facilities and fed different diets. However, the hamsters used in this study were all reared together and fed the same diet, thereby eliminating environmental variability and indicating that the shifts in microbiota are biologically relevant. The present results extend the findings of seasonal shifts in gut microbiota by establishing that the mechanism through which photoperiod alters the gut microbial community includes the pineal gland.

Taxonomic identification in this study was resolved only to the level of genus, as species identification of bacteria can be problematic.[114,115] Although some phyla[116,117] and genera[118,119] have been correlated with specific physiological responses, it is important to note that bacterial species function can vary within the same genus.[120-124] This makes it challenging to form conclusions about the roles of genera as a whole within the microbiota, as well as to reduce the function of the entire microbiota as a system—which

contains trillions of microorganisms[32]—and characterize it by only a handful of community members.[116,125] These points should be carefully considered when analyzing the microbiota and its many potential effects on behavior and physiology.

5 | CONCLUSION

The systems influencing the gut microbiota are numerous and complex, and the circuits and mechanisms subserving communication along the gut-brain axis remain largely uncharacterized. While previous results have identified roles for the immune system and stress axis in host regulation of the gut microbiome, the present study indicates that the pineal gland plays a necessary role in determining the seasonal profile of the microbiota. This opens the door to future chronobiological research aimed at mechanisms driving seasonal rhythms both upstream and downstream of seasonal changes in the gut microbiota. These results also identify a novel mechanism for microbiome researchers to exploit in the area of brain-gut interactions. Pineal MEL signaling may drive shifts in the abundances of gut bacteria, and those shifts in bacteria may, in turn, play a role in the host's seasonal physiological and behavioral responses. These results represent an important advance in our understanding of the relationship between photoperiod, brain, microbiota, and physiology.

ACKNOWLEDGEMENTS

Funding for this study was provided by the Department of Biological Sciences at the University of Memphis. We would like to acknowledge the support from members of the Department of Biological Sciences, Center for Biodiversity Research, and Animal Care Facility at the University of Memphis.

CONFLICTS OF INTEREST

The authors have no conflicts of interest to declare.

AUTHOR CONTRIBUTIONS

Elyan K. Shor and David A. Freeman conceived the study and performed surgical procedures. Shawn P. Brown advised on study design and methods of data analysis. Elyan K. Shor collected weekly samples and measures. Elyan K. Shor and Shawn P. Brown performed molecular work, library preparation, and bioinformatics analyses. All authors wrote, revised, and approved the final manuscript.

ORCID

Elyan K. Shor https://orcid.org/0000-0002-1102-4054
Shawn P. Brown https://orcid.org/0000-0002-4687-1720
David A. Freeman https://orcid.org/0000-0002-9924-9150

REFERENCES

1. Partrick KA, Chassaing B, Beach LQ, McCann KE, Gewirtz AT, Huhman KL. Acute and repeated exposure to social stress reduces gut microbiota diversity in syrian hamsters. *Behav Brain Res*. 2018;345:39-48.
2. Mayer EA, Tillisch K, Gupta A. Gut/brain axis and the microbiota. *J Clin Invest*. 2015;125(3):926-938.
3. Foster JA, Lyte M, Meyer E, Cryan JF. Gut microbiota and brain function: An evolving field in neuroscience. *Int J Neuropsychopharmacol*. 2016;19(5):1-7.
4. Carabotti M, Scirocco A, Maselli MA, Severi C. The gut-brain axis: Interactions between enteric microbiota, central and enteric nervous systems. *Ann Gastroenterol*. 2015;28(2):203-209.
5. Dinan TG, Cryan JF. Melancholic microbes: A link between gut microbiota and depression? *Neurogastroenterol Motil*. 2013;25(9):713-719.
6. Cryan JF, O'Mahony SM. The microbiome-gut-brain axis: From bowel to behavior. *Neurogastroenterol Motil*. 2011;23(3):187-192.
7. Huang EY, Inoue T, Leone VA, et al. Using corticosteroids to reshape the gut microbiome: Implications for inflammatory bowel diseases. *Inflamm Bowel Dis*. 2015;21(5):963-972.
8. Heimesaat MM, Fischer A, Siegmund B, et al. Shift towards pro-inflammatory intestinal bacteria aggravates acute murine colitis via toll-like receptors 2 and 4. *PLoS One*. 2007;2(7):e662.
9. Packey CD, Sartor RB. Commensal bacteria, traditional and opportunistic pathogens, dysbiosis and bacterial killing in inflammatory bowel diseases. *Curr Opin Infect Dis*. 2009;22(3):292-301.
10. Bloom SM, Bijanki VN, Nava GM, et al. Commensal bacteroides species induce colitis in host-genotype-specific fashion in a mouse model of inflammatory bowel disease. *Cell Host Microbe*. 2011;9(5):390-403.
11. Tremaroli V, Backhed F. Functional interactions between the gut microbiota and host metabolism. *Nature*. 2012;489(7415):242-249.
12. Nishino R, Mikami K, Takahashi H, et al. Commensal microbiota modulate murine behaviors in a strictly contamination-free environment confirmed by culture-based methods. *Neurogastroenterol Motil*. 2013;25(6):521-528.
13. Bercik P, Denou E, Collins J, et al. The intestinal microbiota affect central levels of brain-derived neurotropic factor and behavior in mice. *Gastroenterology*. 2011;141(2):599-609.
14. Diaz Heijtz R, Wang S, Anuar F, et al. Normal gut microbiota modulates brain development and behavior. *Proc Natl Acad Sci U S A*. 2011;108(7):3047-3052.
15. Park AJ, Collins J, Blennerhassett PA, et al. Altered colonic function and microbiota profile in a mouse model of chronic depression. *Neurogastroenterol Motil*. 2013;25(9):733.
16. Kelly JR, Borre Y, O'Brien C, et al. Transferring the blues: Depression-associated gut microbiota induces neurobehavioural changes in the rat. *J Psychiatr Res*. 2016;82:109-118.
17. Clarke G, Grenham S, Scully P, et al. The microbiome-gut-brain axis during early life regulates the hippocampal serotonergic system in a sex-dependent manner. *Mol Psychiatry*. 2013;18(6):666-673.
18. Foster JA, McVey Neufeld KA. Gut-brain axis: How the microbiome influences anxiety and depression. *Trends Neurosci*. 2013;36(5):305-312.
19. Crumeyrolle-Arias M, Jaglin M, Bruneau A, et al. Absence of the gut microbiota enhances anxiety-like behavior and neuroendocrine response to acute stress in rats. *Psychoneuroendocrinology*. 2014;42:207-217.

20. de Theije CG, Koelink PJ, Korte-Bouws GA, et al. Intestinal inflammation in a murine model of autism spectrum disorders. *Brain Behav Immun*. 2014;37:240-247.
21. Desbonnet L, Clarke G, Shanahan F, Dinan TG, Cryan JF. Microbiota is essential for social development in the mouse. *Mol Psychiatry*. 2014;19(2):146-148.
22. Arseneault-Breard J, Rondeau I, Gilbert K, et al. Combination of lactobacillus helveticus R0052 and bifidobacterium longum R0175 reduces post-myocardial infarction depression symptoms and restores intestinal permeability in a rat model. *Br J Nutr*. 2012;107(12):1793-1799.
23. Ren CC, Sylvia KE, Munley KM, et al. Photoperiod modulates the gut microbiome and aggressive behavior in siberian hamsters. *J Exp Biol*. 2020;223(3):jeb212548.
24. Sylvia KE, Jewell CP, Rendon NM, St John EA, Demas GE. Sex-specific modulation of the gut microbiome and behavior in siberian hamsters. *Brain Behav Immun*. 2017;60:51-62.
25. Ley RE, Peterson DA, Gordon JI. Ecological and evolutionary forces shaping microbial diversity in the human intestine. *Cell*. 2006;124(4):837-848.
26. Backhed F, Ley RE, Sonnenburg JL, Peterson DA, Gordon JI. Host-bacterial mutualism in the human intestine. *Science*. 2005;307(5717):1915-1920.
27. Bailey MT, Walton JC, Dowd SE, Weil ZM, Nelson RJ. Photoperiod modulates gut bacteria composition in male siberian hamsters (phodopus sungorus). *Brain Behav Immun*. 2010;24(4):577-584.
28. de Lartigue G, Barbier de la Serre C, Espero E, Lee J, Raybould HE. Diet-induced obesity leads to the development of leptin resistance in vagal afferent neurons. *Am J Physiol Endocrinol Metab*. 2011;301(1):E187-E195.
29. Galland L. The gut microbiome and the brain. *J Med Food*. 2014;17(12):1261-1272.
30. Bercik P, Collins SM, Verdu EF. Microbes and the gut-brain axis. *Neurogastroenterol Motil*. 2012;24(5):405-413.
31. Cryan JF, Dinan TG. Mind-altering microorganisms: The impact of the gut microbiota on brain and behaviour. *Nat Rev Neurosci*. 2012;13(10):701-712.
32. Dinan TG, Cryan JF. The microbiome-gut-brain axis in health and disease. *Gastroenterol Clin North Am*. 2017;46(1):77-89.
33. Nelson RJ. Seasonal immune function and sickness responses. *Trends Immunol*. 2004;25(4):187-192.
34. Thaiss CA, Levy M, Korem T, et al. Microbiota diurnal rhythmicity programs host transcriptome oscillations. *Cell*. 2016;167(6):1495-1510.
35. Reber SO. Stress and animal models of inflammatory bowel disease–an update on the role of the hypothalamo-pituitary-adrenal axis. *Psychoneuroendocrinology*. 2012;37(1):1-19.
36. Tannock GW, Savage DC. Influences of dietary and environmental stress on microbial populations in the murine gastrointestinal tract. *Infect Immun*. 1974;9(3):591-598.
37. Spor A, Koren O, Ley R. Unravelling the effects of the environment and host genotype on the gut microbiome. *Nat Rev Microbiol*. 2011;9(4):279-290.
38. Hufeldt MR, Nielsen DS, Vogensen FK, Midtvedt T, Hansen AK. Variation in the gut microbiota of laboratory mice is related to both genetic and environmental factors. *Comp Med*. 2010;60(5):336-347.
39. Voigt RM, Forsyth CB, Green SJ, et al. Circadian disorganization alters intestinal microbiota. *PLoS One*. 2014;9(5):e97500.
40. Stevenson TJ, Prendergast BJ. Photoperiodic time measurement and seasonal immunological plasticity. *Front Neuroendocrinol*. 2015;37:76-88.
41. Weil ZM, Borniger JC, Cisse YM, Abi Salloum BA, Nelson RJ. Neuroendocrine control of photoperiodic changes in immune function. *Front Neuroendocrinol*. 2015;37:108-118.
42. Walton JC, Weil ZM, Nelson RJ. Influence of photoperiod on hormones, behavior, and immune function. *Front Neuroendocrinol*. 2011;32(3):303-319.
43. Wen JC, Prendergast BJ. Photoperiodic regulation of behavioral responsiveness to proinflammatory cytokines. *Physiol Behav*. 2007;90(5):717-725.
44. Prendergast BJ, Yellon SM, Tran LT, Nelson RJ. Photoperiod modulates the inhibitory effect of in vitro melatonin on lymphocyte proliferation in female siberian hamsters. *J Biol Rhythms*. 2001;16(3):224-233.
45. Duncan MJ, Goldman BD. Hormonal regulation of the annual pelage color cycle in the djungarian hamster, phodopus sungorus. I. role of the gonads and pituitary. *J Exp Zool*. 1984;230(1):89-95.
46. Wade GN, Bartness TJ. Effects of photoperiod and gonadectomy on food intake, body weight, and body composition in siberian hamsters. *Am J Physiol*. 1984;246(1 Pt 2):R26-30.
47. Goldman BD. Parameters of the circadian rhythm of pineal melatonin secretion affecting reproductive responses in siberian hamsters. *Steroids*. 1991;56(5):218-225.
48. Jasnow AM, Huhman KL, Bartness TJ, Demas GE. Short-day increases in aggression are inversely related to circulating testosterone concentrations in male siberian hamsters (phodopus sungorus). *Horm Behav*. 2000;38(2):102-110.
49. Carter DS, Goldman BD. Antigonadal effects of timed melatonin infusion in pinealectomized male djungarian hamsters (phodopus sungorus sungorus): Duration is the critical parameter. *Endocrinology*. 1983;113(4):1261-1267.
50. Wen JC, Dhabhar FS, Prendergast BJ. Pineal-dependent and -independent effects of photoperiod on immune function in siberian hamsters (phodopus sungorus). *Horm Behav*. 2007;51(1):31-39.
51. Goldman BD. Mammalian photoperiodic system: Formal properties and neuroendocrine mechanisms of photoperiodic time measurement. *J Biol Rhythms*. 2001;16(4):283-301.
52. Prendergast BJ, Freeman DA. Pineal-independent regulation of photo-nonresponsiveness in the siberian hamster (phodopus sungorus). *J Biol Rhythms*. 1999;14(1):62-71.
53. Freeman DA, Kampf-Lassin A, Galang J, Wen JC, Prendergast BJ. Melatonin acts at the suprachiasmatic nucleus to attenuate behavioral symptoms of infection. *Behav Neurosci*. 2007;121(4):689-697.
54. Caporaso JG, Lauber CL, Walters WA, et al. Global patterns of 16S rRNA diversity at a depth of millions of sequences per sample. *Proc Natl Acad Sci USA*. 2011;108(Suppl 1):4516-4522.
55. Brown SP, Leopold DR, Busby PE. Protocols for investigating the leaf mycobiome using high-throughput DNA sequencing. *Methods Mol Biol*. 2018;1848:39-51.
56. Brown SP, Veach AM, Horton JL, Ford E, Jumpponen A, Baird R. Context dependent fungal and bacterial soil community shifts in response to recent wildfires in the southern appalachian mountains. *For Ecol Manage*. 2019;451:117520.
57. Brown SP, Jumpponen A. Contrasting primary successional trajectories of fungi and bacteria in retreating glacier soils. *Mol Ecol*. 2014;23(2):481-497.

58. Schloss PD, Westcott SL, Ryabin T, et al. Introducing mothur: Open-source, platform-independent, community-supported software for describing and comparing microbial communities. *Appl Environ Microbiol*. 2009;75(23):7537-7541.
59. Kozich JJ, Westcott SL, Baxter NT, Highlander SK, Schloss PD. Development of a dual-index sequencing strategy and curation pipeline for analyzing amplicon sequence data on the MiSeq illumina sequencing platform. *Appl Environ Microbiol*. 2013;79(17):5112-5120.
60. Martin M. Cutadapt removes adapter sequences from high-throughput sequencing reads. *EMBnet.journal*. 2011;17(1):10-12.
61. Huse SM, Welch DM, Morrison HG, Sogin ML. Ironing out the wrinkles in the rare biosphere through improved OTU clustering. *Environ Microbiol*. 2010;12(7):1889-1898.
62. Rognes T, Flouri T, Nichols B, Quince C, Mahe F. VSEARCH: A versatile open source tool for metagenomics. *PeerJ*. 2016;4:e2584.
63. Wang Q, Garrity GM, Tiedje JM, Cole JR. Naive bayesian classifier for rapid assignment of rRNA sequences into the new bacterial taxonomy. *Appl Environ Microbiol*. 2007;73(16):5261-5267.
64. Westcott SL, Schloss PD. OptiClust, an improved method for assigning amplicon-based sequence data to operational taxonomic units. *mSphere*. 2017;2(2):e00073-17.
65. Brown SP, Veach AM, Rigdon-Huss AR, et al. Scraping the bottom of the barrel: are rare high throughput sequences artifacts? *Fungal Ecology*. 2015;13:221-225.
66. Oliver AK, Brown SP, Callaham MA, Jumpponen A. Polymerase matters: non-proofreading enzymes inflate fungal community richness estimates by up to 15 %. *Fungal Ecology*. 2015;15:86-89.
67. Anderson MJ. A new method for non-parametric multivariate analysis of variance. *Austral Ecol*. 2001;26(1):32-46.
68. Furet JP, Kong LC, Tap J, et al. Differential adaptation of human gut microbiota to bariatric surgery-induced weight loss: Links with metabolic and low-grade inflammation markers. *Diabetes*. 2010;59(12):3049-3057.
69. Kaczmarek JL, Musaad SM, Holscher HD. Time of day and eating behaviors are associated with the composition and function of the human gastrointestinal microbiota. *Am J Clin Nutr*. 2017;106(5):1220-1231.
70. Liang X, Bushman FD, FitzGerald GA. Rhythmicity of the intestinal microbiota is regulated by gender and the host circadian clock. *Proc Natl Acad Sci U S A*. 2015;112(33):10479-10484.
71. Turnbaugh PJ, Hamady M, Yatsunenko T, et al. A core gut microbiome in obese and lean twins. *Nature*. 2009;457(7228):480-484.
72. Segata N, Izard J, Waldron L, et al. Metagenomic biomarker discovery and explanation. *Genome Biol*. 2011;12(6):R60-2011.
73. Benjamini Y, Hochberg Y. Controlling the False Discovery Rate: A Practical and Powerful Approach to Multiple Testing. *J R Stat Soc: Series B*. 1995;57(1):289-300.
74. Ohara T. Identification of the microbial diversity after fecal microbiota transplantation therapy for chronic intractable constipation using 16s rRNA amplicon sequencing. *PLoS One*. 2019;14(3):e0214085.
75. Kovatcheva-Datchary P, Nilsson A, Akrami R, et al. Dietary fiber-induced improvement in glucose metabolism is associated with increased abundance of prevotella. *Cell Metab*. 2015;22(6):971-982.
76. Dillon SM, Lee EJ, Kotter CV, et al. Gut dendritic cell activation links an altered colonic microbiome to mucosal and systemic T-cell activation in untreated HIV-1 infection. *Mucosal Immunol*. 2016;9(1):24-37.
77. Scher JU, Sczesnak A, Longman RS, et al. Expansion of intestinal prevotella copri correlates with enhanced susceptibility to arthritis. *Elife*. 2013;2:e01202.
78. Gupta VK, Chaudhari NM, Iskepalli S, Dutta C. Divergences in gene repertoire among the reference prevotella genomes derived from distinct body sites of human. *BMC Genom*. 2015;16:153.
79. Zhu A, Sunagawa S, Mende DR, Bork P. Inter-individual differences in the gene content of human gut bacterial species. *Genome Biol*. 2015;16:82.
80. Ottman N, Smidt H, de Vos WM, Belzer C. The function of our microbiota: Who is out there and what do they do? *Front Cell Infect Microbiol*. 2012;2:104.
81. Ramakrishna BS. Role of the gut microbiota in human nutrition and metabolism. *J Gastroenterol Hepatol*. 2013;28(Suppl 4):9-17.
82. Tolhurst G, Heffron H, Lam YS, et al. Short-chain fatty acids stimulate glucagon-like peptide-1 secretion via the G-protein-coupled receptor FFAR2. *Diabetes*. 2012;61(2):364-371.
83. Samuel BS, Shaito A, Motoike T, et al. Effects of the gut microbiota on host adiposity are modulated by the short-chain fatty-acid binding G protein-coupled receptor, Gpr41. *Proc Natl Acad Sci U S A*. 2008;105(43):16767-16772.
84. Backhed F, Manchester JK, Semenkovich CF, Gordon JI. Mechanisms underlying the resistance to diet-induced obesity in germ-free mice. *Proc Natl Acad Sci U S A*. 2007;104(3):979-984.
85. Rinninella E, Raoul P, Cintoni M, et al. What is the healthy gut microbiota composition? A changing ecosystem across age, environment, diet, and diseases. *Microorganisms*. 2019;7(1):14.
86. Castaner O, Goday A, Park YM, et al. The gut microbiome profile in obesity: A systematic review. *Int J Endocrinol*. 2018;2018:4095789.
87. Ley RE. Obesity and the human microbiome. *Curr Opin Gastroenterol*. 2010;26(1):5-11.
88. Bao R, Onishi KG, Tolla E, et al. Genome sequencing and transcriptome analyses of the siberian hamster hypothalamus identify mechanisms for seasonal energy balance. *Proc Natl Acad Sci U S A*. 2019;116(26):13116-13121.
89. Ebling FJ, Barrett P. The regulation of seasonal changes in food intake and body weight. *J Neuroendocrinol*. 2008;20(6):827-833.
90. Bartness TJ, Wade GN. Photoperiodic control of seasonal body weight cycles in hamsters. *Neurosci Biobehav Rev*. 1985;9(4):599-612.
91. El Aidy S, Dinan TG, Cryan JF. Gut microbiota: The conductor in the orchestra of immune-neuroendocrine communication. *Clin Ther*. 2015;37(5):954-967.
92. Grenham S, Clarke G, Cryan JF, Dinan TG. Brain-gut-microbe communication in health and disease. *Front Physiol*. 2011;2:94.
93. Capuco A, Urits I, Hasoon J, et al. Current perspectives on gut microbiome dysbiosis and depression. *Adv Ther*. 2020;37:1328-1346.
94. Bienenstock J, Kunze W, Forsythe P. Microbiota and the gut-brain axis. *Nutr Rev*. 2015;73(Suppl 1):28-31.
95. Liang S, Wu X, Jin F. Gut-brain psychology: Rethinking psychology from the microbiota-gut-brain axis. *Front Integr Neurosci*. 2018;12:33.
96. Teichman EM, O'Riordan KJ, Gahan CGM, Dinan TG, Cryan JF. When rhythms meet the blues: Circadian interactions with the microbiota-gut-brain axis. *Cell Metab*. 2020;31(3):448-471.

97. Leone V, Gibbons SM, Martinez K, et al. Effects of diurnal variation of gut microbes and high-fat feeding on host circadian clock function and metabolism. *Cell Host Microbe*. 2015;17(5):681-689.
98. Thaiss CA, Zeevi D, Levy M, et al. Transkingdom control of microbiota diurnal oscillations promotes metabolic homeostasis. *Cell*. 2014;159(3):514-529.
99. Zarrinpar A, Chaix A, Yooseph S, Panda S. Diet and feeding pattern affect the diurnal dynamics of the gut microbiome. *Cell Metab*. 2014;20(6):1006-1017.
100. Weger BD, Gobet C, Yeung J, et al. The mouse microbiome is required for sex-specific diurnal rhythms of gene expression and metabolism. *Cell Metab*. 2019;29(2):362-382.
101. Tahara Y, Yamazaki M, Sukigara H, et al. Gut microbiota-derived short chain fatty acids induce circadian clock entrainment in mouse peripheral tissue. *Sci Rep*. 2018;8(1):1395-2018.
102. Montagner A, Korecka A, Polizzi A, et al. Hepatic circadian clock oscillators and nuclear receptors integrate microbiome-derived signals. *Sci Rep*. 2016;6:20127.
103. Mukherji A, Kobiita A, Ye T, Chambon P. Homeostasis in intestinal epithelium is orchestrated by the circadian clock and microbiota cues transduced by TLRs. *Cell*. 2013;153(4):812-827.
104. Bubenik GA. Gastrointestinal melatonin: Localization, function, and clinical relevance. *Dig Dis Sci*. 2002;47(10):2336-2348.
105. Acuna-Castroviejo D, Escames G, Venegas C, et al. Extrapineal melatonin: Sources, regulation, and potential functions. *Cell Mol Life Sci*. 2014;71(16):2997-3025.
106. Paulose JK, Cassone VM. The melatonin-sensitive circadian clock of the enteric bacterium enterobacter aerogenes. *Gut Microbes*. 2016;7(5):424-427.
107. Paulose JK, Wright JM, Patel AG, Cassone VM. Human gut bacteria are sensitive to melatonin and express endogenous circadian rhythmicity. *PLoS One*. 2016;11(1):e0146643.
108. Bubenik GA, Brown GM. Pinealectomy reduces melatonin levels in the serum but not in the gastrointestinal tract of rats. *Biol Signals*. 1997;6(1):40-44.
109. Vakkuri O, Rintamaki H, Leppaluoto J. Plasma and tissue concentrations of melatonin after midnight light exposure and pinealectomy in the pigeon. *J Endocrinol*. 1985;105(2):263-268.
110. Bubenik GA, Hacker RR, Brown GM, Bartos L. Melatonin concentrations in the luminal fluid, mucosa, and muscularis of the bovine and porcine gastrointestinal tract. *J Pineal Res*. 1999;26(1):56-63.
111. Reiter RJ, Rosales-Corral S, Coto-Montes A, et al. The photoperiod, circadian regulation and chronodisruption: The requisite interplay between the suprachiasmatic nuclei and the pineal and gut melatonin. *J Physiol Pharmacol*. 2011;62(3):269-274.
112. Tsukamoto K, Ariga H, Mantyh C, et al. Luminally released serotonin stimulates colonic motility and accelerates colonic transit in rats. *Am J Physiol Regul Integr Comp Physiol*. 2007;293(1):R64-R69.
113. Bubenik GA. The effect of serotonin, N-acetylserotonin, and melatonin on spontaneous contractions of isolated rat intestine. *J Pineal Res*. 1986;3(1):41-54.
114. Cohan FM. What are bacterial species? *Annu Rev Microbiol*. 2002;56:457-487.
115. Margos G, Fingerle V, Cutler S, Gofton A, Stevenson B, Estrada-Pena A. Controversies in bacterial taxonomy: The example of the genus borrelia. *Ticks Tick Borne Dis*. 2020;11(2):101335.
116. Johnson EL, Heaver SL, Walters WA, Ley RE. Microbiome and metabolic disease: Revisiting the bacterial phylum bacteroidetes. *J Mol Med (Berl)*. 2017;95(1):1-8.
117. Lopetuso LR, Scaldaferri F, Petito V, Gasbarrini A. Commensal clostridia: Leading players in the maintenance of gut homeostasis. *Gut Pathog*. 2013;5(1):23-4749.
118. Beller A, Kruglov A, Durek P, et al. P104 Anaeroplasma, a potential anti-inflammatory probiotic for the treatment of chronic intestinal inflammation. *Ann Rheum Dis*. 2019;78(Suppl 1):A45-A46.
119. Ozato N, Saito S, Yamaguchi T, et al. Blautia genus associated with visceral fat accumulation in adults 20–76 years of age. *NPJ Biofilms Microbiomes*. 2019;5:28-019.
120. Menard A, Smet A. Review: Other helicobacter species. *Helicobacter*. 2019;24(Suppl 1):e12645.
121. Million M, Angelakis E, Paul M, Armougom F, Leibovici L, Raoult D. Comparative meta-analysis of the effect of lactobacillus species on weight gain in humans and animals. *Microb Pathog*. 2012;53(2):100-108.
122. Lefebure T, Stanhope MJ. Pervasive, genome-wide positive selection leading to functional divergence in the bacterial genus campylobacter. *Genome Res*. 2009;19(7):1224-1232.
123. Ryan RP, Monchy S, Cardinale M, et al. The versatility and adaptation of bacteria from the genus stenotrophomonas. *Nat Rev Microbiol*. 2009;7(7):514-525.
124. Canchaya C, Claesson MJ, Fitzgerald GF, van Sinderen D, O'Toole PW. Diversity of the genus lactobacillus revealed by comparative genomics of five species. *Microbiology*. 2006;152(Pt 11):3185-3196.
125. Koren O, Knights D, Gonzalez A, et al. A guide to enterotypes across the human body: Meta-analysis of microbial community structures in human microbiome datasets. *PLoS Comput Biol*. 2013;9(1):e1002863.

SUPPORTING INFORMATION

Additional supporting information may be found online in the Supporting Information section.

How to cite this article: Shor EK, Brown SP, Freeman DA. A novel role for the pineal gland: Regulating seasonal shifts in the gut microbiota of Siberian hamsters. *J Pineal Res.* 2020;69:e12696. https://doi.org/10.1111/jpi.12696